Int. J. Heat Mass Transfer. Vol. 14, pp. 1433–1443. Pergamon Press 1971. Printed in Great Britain

MEASUREMENTS ON IONIZED NITROGEN IN JETS AND ESTIMATIONS OF PRANDTL NUMBER

D. J. MYRONUK† **and S. L. SOO**

Department of Mechanical Engineering, University of Illinois, Urbana, Illinois 61801, U.S.A.

(*Received* 10 *November* 1969 *and in revised form* 11 *November* 1970)

Abstract—Measurement of temperatures and electron densities of a free jet of ionized nitrogen at atmospheric pressure were made by a spectroscopic method. The gas temperatures were in the range of 9000–15000°K and the electron densities were in the range of $5 \times 10^{15}/cm^3$–$10^{17}/cm^3$. Nitrogen mass flow rates were 0·05 and 0·1 g/s with arc currents of 200 and 300 A at 40V. An estimation of Prandtl numbers was made from the temperature distribution in the jet, giving values ranging from 0·06 to 0·75.

1. INTRODUCTION

JETS of ionized gases at high temperatures have been used in industrial processes, in research and testing, and in energy conversion and propulsion. In all these applications, information of distributions of temperature and electron density in the jet plume and data such as transport properties of the gas in a jet are useful. In the present study measurements of temperatures and electron densities were made on a free jet of ionized nitrogen at atmospheric pressure produced by a high current arc heater. These measurements were made by plasma spectroscopy as outlined in the treatise of Griem [1] and recent studies of Robinson and Lenn [2]. The data were correlated according to the basic relations of jet and separated flow and the associated transported processes under the influence of recombination.

2. DISSOCIATION AND IONIZATION

At atmospheric pressure and at temperatures below 15000°K the basic reactions in ionized nitrogen and the energy required are [3,4]

$$e + N_2 \rightarrow N_2^+ + e + e \qquad 15{\cdot}58 \text{ e.v.} \quad (1)$$

$$e + N_2 \rightarrow N^+ + N + e + e \qquad 24{\cdot}33 \text{ e.v.} \quad (2)$$

$$e + N_2^+ \rightarrow N^+ + N + e \qquad 8{\cdot}73 \text{ e.v.} \quad (3)$$

$$e + N + N \rightarrow N_2 + e \qquad -9{\cdot}76 \text{ e.v.} \quad (4)$$

The occurrence of non-equilibrium states, i.e. the metastable and excited states of ions, atoms, and molecules, are negligible at the low flow velocities in the present study. Reactions of any of the species with the materials constituting the electrodes were also shown to be negligible. Further, the concentrations of N^{++} and N^{+++} in ionized nitrogen gas at atmospheric pressure is far smaller than those of N, N_2^+ and N^+ at temperatures below 15000°K.

For a diatomic gas in large spatial gradients, non-equilibrium results from the relaxation times associated with the adjustment and distribution on internal energy among the translation, rotation, vibration, electronic, and chemical states of a given particle. If the gradients are so large that the particles cannot adjust their internal energy to the surroundings over distances of a few mean free paths, the concept of local thermodynamic equilibrium (LTE) cannot be applied. However, McGregor [5] showed that the dense plasmas such gradients are seldom observed and a Maxwellian distribution is

† Present address: Department of Mechanical Engineering, San Jose State College, San Jose, California 95114, U.S.A.

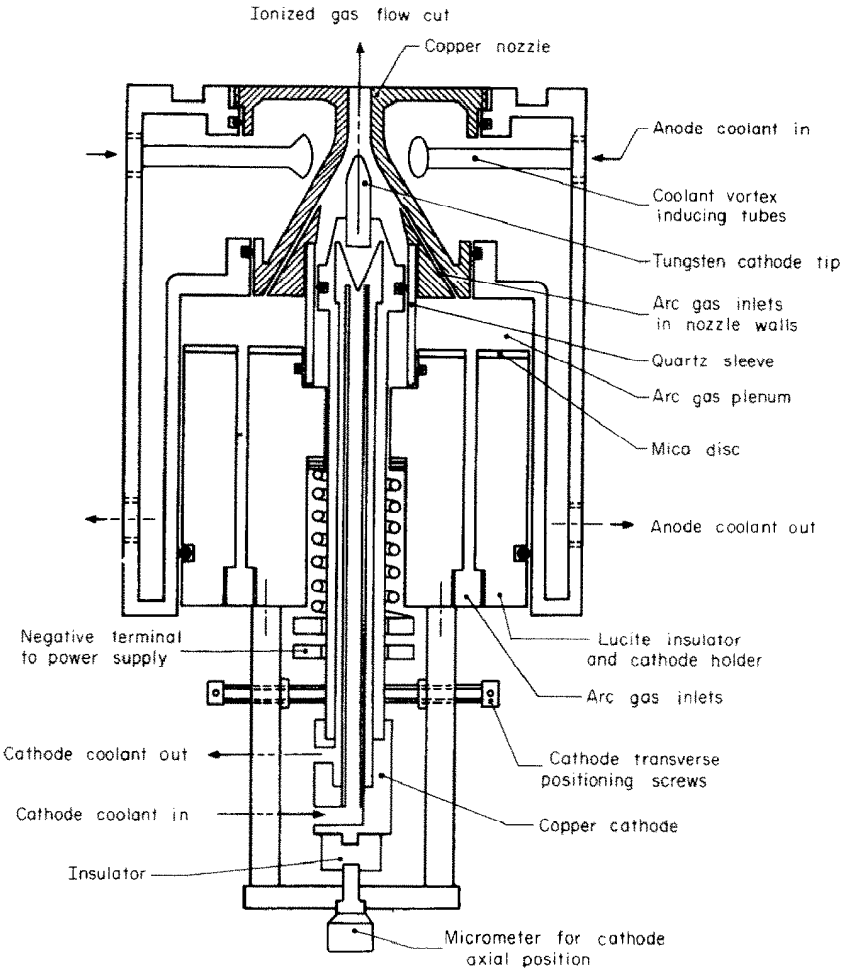

FIG. 1. Plasma generator.

always assured. Moreover, the vibration relaxation time is a rapidly decreasing function of temperature [6]. To insure LTE in an optically thin ionized gas, it is necessary that among collision processes in an arc discharge the electron collisions are mainly responsible for the distribution of electronic states [8], electron density greater than 10^{16} cm^{-3} assures LTE [1,7,8].

The conditions of LTE are satisfied in this study because of the high temperature and sufficiently high electron concentrations. In addition, it is readily shown that real gas effects due to interaction between particles [9], particles with radiation [10], and lowering of ionization potential by polarization [11] are negligible in the range of the present study.

3. EXPERIMENTAL APPARATUS

The plasma jet shown in Fig. 1 was used to produce an external-field-free plasma column with temperatures in the neighborhood of 15000°K, depending on the power input, the gas used, and the mass flow rate of the gas. The freely expanding jet exhausted to atmospheric pressure in a downstream observation chamber

that was open to surrounding stagnant air. The arc jet nozzle converged at an angle of 60° to a throat diameter of slightly less than 5 mm and diverged slightly to an exit diameter of 5 mm. The nozzle anode was made out of copper while the cathode consisted of a water cooled, 1/4-in. 2% thoriated tungsten rod.

The arc power was furnished by A. O. Smith welders provided up to 20 kW with a current range of 100–400 A. Nitrogen flow rates could be varied from 0·01 to 0·5 g/s at S.T.P.

The high current arc discharge was stabilized by a cooled, copper-walled, slightly divergent section of the jet nozzle. Wall stabilization [12] in this study is preferred to vortex stabilization for producing an axisymmetric intensity distribution.

The copper nozzle wall-thickness was 3 mm and the inner wall temperature at the exit did not exceed 600°K. Coolant flow rates were 20·0 kg/min to the anode and 3·6 kg/min to the cathode. The cooling water was injected at high velocity through a tangential arrangement of feeder tubes as shown in Fig. 1. The copper anode was easily removed for cleaning and inspection. Ablation of the inner surface of the nozzle was negligible (< 0·1% by weight of the nozzle) during the first 5 h of operation although the green copper spectra was visible in the exhaust plume.

4. FREE JET OF AN IONIZED GAS

The initial condition of a free jet of ionized gas is given by non-equilibrium nozzle flow at sonic velocity consisting of a merging weak-shock structure with a surface viscous layer of relaxing, dissociating ionized gas [13]. Various mutual and self interactions of electron, ion, atoms, and molecules occur. The mechanisms of these interactions include diffusion, recombination [14], induced drift velocities [15], and non-equilibrium radiation [16]. At low velocities in this study, frozen compositions [17] did not occur and chemical reactions, other than recombinations, were negligible.

The exit condition from a nozzle to an enlarged volume gave the initial condition of a free jet. The arc jet used in this study was operated only in the subsonic velocity range within which there were three flow regimes specified as laminar, transition, or turbulent as delineated in the diagrams of Fig. 2.

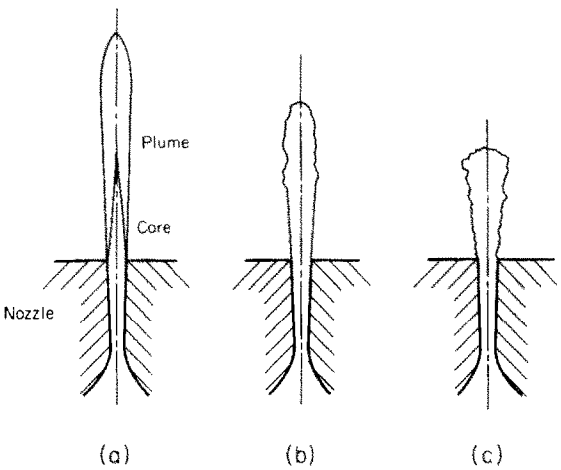

FIG. 2. Visual description of laminar, transition and turbulent flow of a plasma jet.
(a) Acoustically quiet, long luminous plume, intensely bright core, core length of several orifice diameters. Plume length of 1–10 core lengths, $50 < N_{Re} < 200$, all boundaries were smooth. (b) Some audible noise, no observable plume, intensely bright core, core, length of several orifice diameters, $200 < N_{Re} < 400$, all boundaries were initially smooth, became ragged downstream. (c) Acoustically noisy, no observable plume, intensely bright core, core length of a few orifice diameters, $N_{Re} > 400$, all boundaries were ragged.

In the laminar mode, an arc jet was seen to have three distinct features: (a) there was an intensely bright core several diameters long at the nozzle exit; (b) beyond the core, there was a much longer and less intense luminous plume; (c) the edges of the plume and core were perceptibly smooth. We refer to the case where there is a stable plume as a jet operating in a laminar mode.

In transition mode flow regime, no plume was visible above the intense core region. Although the jet boundary was smooth following emergence from the nozzle exit, about three to five diameters downstream mixing occurred, and the

boundary of plasma became ragged prior to joining at the jet axis. The process became audible. Operation in turbulent mode was characterized by a total observable jet length of only a few diameters; the boundary layer was markedly ragged from the nozzle exit to the joining point on the axis, and the jet was quite noisy. The laminar mixing zone length was at least twice the mixing zone length associated with a turbulent shear layer. Our measurements were made only over the range where stable laminar mode existed.

The above ranges were characterized by the Reynolds number N_{Re} based on the orifice diameter and bulk jet properties, and is defined as:

$$N_{Re} = \frac{(2r_1)\rho v}{\mu} = \frac{2\dot{m}}{\pi r_1 \mu} \tag{5}$$

where $\dot{m}$ is the gas flow rate, $2r_1$ is the orifice diameter, v is jet velocity, ρ and μ are the density and viscosity respectively of the gas evaluated at the average jet temperature. $N_{Re} < 200$ for the laminar mode.

The near jet condition can be represented by the relation of separated flow of Görtler. [18] who gave the axial velocity u of free jet as:

$$u = \frac{u_0}{2}\left\{1 + \operatorname{erf}\xi\right\} \tag{6}$$

for flow into a stagnant fluid medium; u_0 is the velocity of the core of the jet. For the present system, $\xi = \sigma(r_0 - r)/z$, σ is a similarity parameter, r_0 is in the radius at which $u = u_0/2$, r is the radius, and z is the axial location from the exit of the nozzle. Equation (6) is valid for the high temperature jet at low Mach numbers because of small compressibility effects, Szablewsky [18] showed that the widths of the mixing gases are affected only very slightly by a large variation in density. The diameter of the jet renders it a thin emitter [24]; heat loss and temperature change by radiation is negligible and hence the change of electron density in the core. It is expected that the condition of LTE is satisfied in the core but not at the boundary where electron density is controlled by diffusion. It is readily shown that for a jet of an ionized gas, the distribution of electron density is given by [19]

$$n_e = (n_{e0}/2)\{1 + \operatorname{erf}[\sqrt{(N_{Sc})}\xi]\} \tag{7}$$

where n_{e0} is the electron density in the core, N_{Sc} is the Schmidt number for electron diffusion. For mixing in separated flow, we have $N_{Sc} \sim 1$, which we shall confirm also from the known value of σ [20],

$$\sigma \sim 12 + 2{\cdot}758\frac{u_0^*}{\sqrt{\left[\left(1 - u_0^{*2}\right)\left(\frac{\gamma - 1}{2}\right)\right]}} \tag{8}$$

when $u_0^* = u_0/\sqrt{(2c_pT_0)}$ whose c_p is the specific heat at constant pressure and T_0 is the core temperature. A similar integration procedure as that leading to equation (7) gave the temperature distribution in the jet as:

$$T = \frac{T_0 + T_\infty}{2}\left\{1 + \frac{T_0 - T_\infty}{T_0 + T_\infty} \times \operatorname{erf}\left[\sqrt{(N_{Pr})}\xi\right]\right\}. \tag{9}$$

When N_{Pr} is the Prandtl number of the gas, T_0 is the core temperature and T_∞ temperature of the surrounding air (500°K), r_0 is the radius at which $T = (T_0 + T_\infty)/2$. Equation (9) permits us to make an estimation of N_{Pr} from measured temperature distributions. Equation (9) is valid because the effect of thermal diffusion is small. The effect of ionization on Prandtl number is principally via its effect on thermal conductivity. Over the width of the mixing, the conditions of both near LTE of the core and non-equilibrium at the boundary are felt. However, because of the sharp temperature drop over the mixing width, the principal influence is that of the temperature distribution in the core region and is therefore near LTE as specified in [23].

The far jet condition, that is, at large distance from the exit of the orifice [21], is represented by the relation of Schlichting and Tollmein [18].

Following the integration procedure of Soo [21] for the distribution of density, we get

$$\frac{T - T_\infty}{T_0 - T_\infty} = C\frac{\gamma r_1}{z}\left(1 + \frac{\gamma^2 r^2}{4z^2}\right)^{-2N_{Pr}} \qquad (10)$$

when r_1 is the radius of the orifice, $\gamma = (\sqrt{3}/8)N_{Re}$ and the coefficient C is a function of N_{Pr},

N_{Pr}	1/2	3/4	1	2	15/4
C	$\frac{1}{\pi\sqrt{3}}$	$\frac{1}{2\sqrt{3}}$	$\frac{2}{\pi\sqrt{3}}$	$\frac{16}{5\pi\sqrt{3}}$	$\frac{3003}{2008\sqrt{3}}$

Equation (10) permits an estimation on N_{Pr} at far downstream from the orifice.

5. SPECTROSCOPIC METHOD

The determination of electron density using hydrogen gas as a tracer according to the method of Griem based on Balmer line broadening [1] was applicable to an argon plasma [22]. Its application to a nitrogen plasma jet is more difficult and has questionable validity when multiple species and recombination processes are present. Thus the available procedures are those based on line radiation and continuum radiation.

Line radiation [1,2,23] usually offers a convenient method for the measurement of temperatures and species [24]. However, in the present study reliability of temperature determined from the ratio of ion/atom (3995Å/4137·6 Å) lines suffered from the scatter in the spectrometer output. This was also because of the proximity of the persistent tungsten line at 4008 Å. Moreover, the values of transition probability of these lines and 4935 Å are not accurately known [25]. Therefore, measurements based on continuum radiation appeared to be most promising.

Continuum radiation is the result of free–free (Bremsstrahlung) and free-bound transitions of free electrons in the ionized gas. The free–bound radiation is given by [23]

$$I_{fb} = h\nu + \text{K.E.} \qquad (11)$$

where h is the Planck constant, ν is the frequency, K.E. is the kinetic energy of the electron before capture. Since translational energy is continuous, both types of radiation give a continuous emission spectra. Individual equations for these radiations given by Huddlestone and Leonard [8] were combined and summed over internal energy levels to give, according to the Kramers–Unsöld theory [26–28]

$$I_{c\lambda} = (5{\cdot}41 \times 10^{-46}\, c\bar{g}n_e^2)/(\lambda T_e^{\frac{1}{2}}) \qquad (12)$$

for the singly ionized gas where the intensity I_λ is in (W cm^{-3} – sr^{-1} – $\Delta\lambda$), c is the speed of light in cm s^{-1}, λ is the wave length in cm; n_e is the electron number density, T_e is the electron temperature, and g is the quantum mechanical Gaunt factor (−1 for hydrogen). Equation (12) gave the temperatures vs. relative intensities; the electron number density was given [29,30] by the Saha equation for ionization [31].

6. EXPERIMENTAL PROCEDURE

The plasma jet was produced by an arc at a given nitrogen flow rate, power input, and electrode spacing with maximum cooling water flow. A reading of plume centerline intensity was recorded on a photomultiplier microphotometer. This value of intensity was reasonably steady and after long test periods, small deviations due to minor ablation of the electrodes were compensated for by making a very slight change in the cathode position, current input or both.

Three minutes were allowed for thermal stabilization of the system and experimental runs were always made starting from the minimum power input and gas flow and increasing these parameters. When the control intensity, I_c, on the microphotometer became steady, a scanning with the Jarrell Ash spectrometer was made. The spectrometer was mounted on a heavy steel frame that was indexed in a vertical sense, parallel to the jet axis, using a hydraulic cylinder. In addition, the spectrometer was indexed in the horizontal plane by a motor driven screw device that allowed very precise positioning transverse to the plasma jet column. An image of the region of the exhaust plume being observed was focused

on the spectrometer slit with a combination of front surfaced spherical and plane mirrors.

The spectrometer scanning pattern normal to the jet axis ("side on") was as follows: starting on the plasma jet centerline, one millimeter downstream from the nozzle exit, a plume radius scan was performed with the spectrometer set at a particular spectral line value of the nitrogen continuum at 4955 Å. The spectrometer response to the emission of the calibrated tungsten ribbon lamp was also recorded. This procedure was followed for nitrogen flow rates of 0·05 and 0·1 g/s at arc currents of 200 and 300 A. The whole spectrometer and optical system was lowered 1·3, 2·5 and 3·8 cm and the process repeated.

Following spectrometer observations, a tungsten shielded chromel–alumel thermocouple was driven radially to the edge of the plasma column at various distances from the nozzle exit plane. The thermocouple was also driven to the centerline of the exhaust plume as close as possible to the apparent end of the plume.

The output of the spectrometer consisted of curves of emission intensity versus radius at several positions transverse to the plasma column at various axial distances. The profiles of 4955 Å continuum were converted to radial intensities by using the Abel integral formulation [32] which gave maximum radial values of intensity for each wavelength. The radial relative intensity ratios were calculated and these values

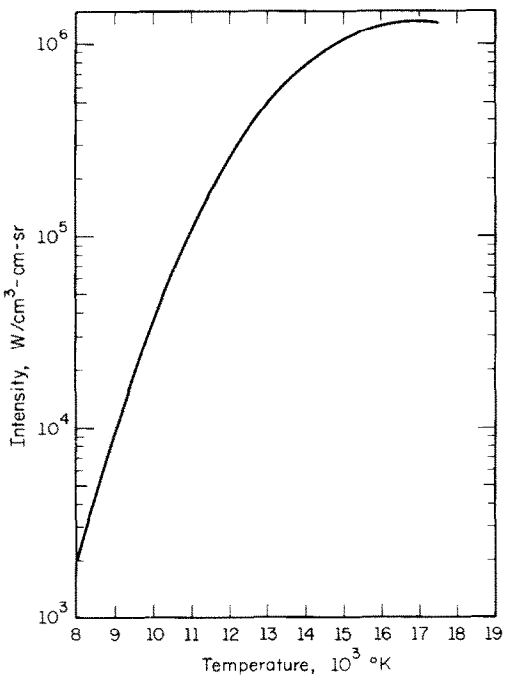

FIG. 3. Continuum intensity for nitrogen at 4955 Å vs. temperature (p = 1 atm).

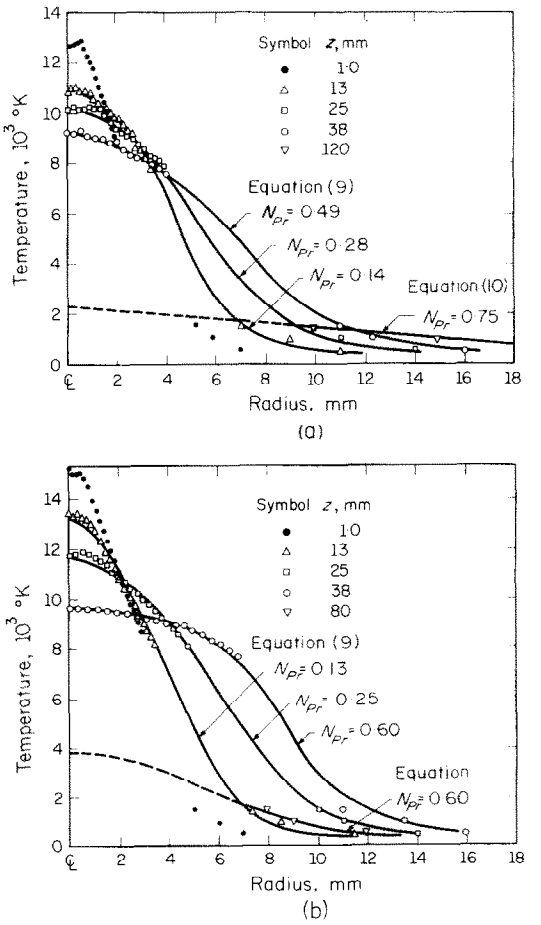

FIG. 4. Radial temperature profiles of nitrogen jet at various axial locations from nozzle exit; curves of equation (9) are based on σ = 12; P = 1 atm.
(a) $\dot{m}$ = 0·05 g/s, I = 200 A, V = 38 V.
(b) $\dot{m}$ = 0·10 g/s, I = 300 A, V = 40 V.

were used in Fig. 3 to determine temperatures [33]. The background intensities were subtracted from the initially observed integrated profiles.

"End-on" observations, made by looking axially back toward the nozzle exit from a position downstream gave maximum radial temperatures near the nozzle exit, were independent of axial distance.

7. EXPERIMENTAL RESULTS

The "side-on" radial temperature profiles illustrated in Fig. 4 and the electron density profiles, illustrated in Fig. 5 are all based on observations of nitrogen 4955 Å continuum. For the 4955 Å line, where the spectrometer was calibrated absolutely against the tungsten ribbon lamp, the area under the line rather than a maximum value was required.

A source of emission intensity fluctuation involved the geometry of the cathode tip. After a few trials, the $\frac{1}{4}$ in. dia., 2% thoriated tungsten rod was initially ground and polished to a 1 mm radius on the conical tip. the arc was uniformly confined in the anode, the exhaust plume inten-

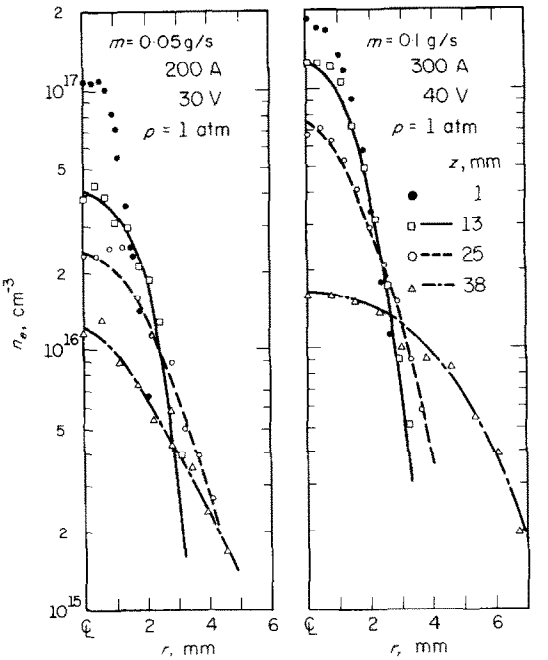

FIG. 5. Radial distribution of electron density. Curves are for $N_{Sc} = 1$ of electron diffusion, $\sigma = 12$.

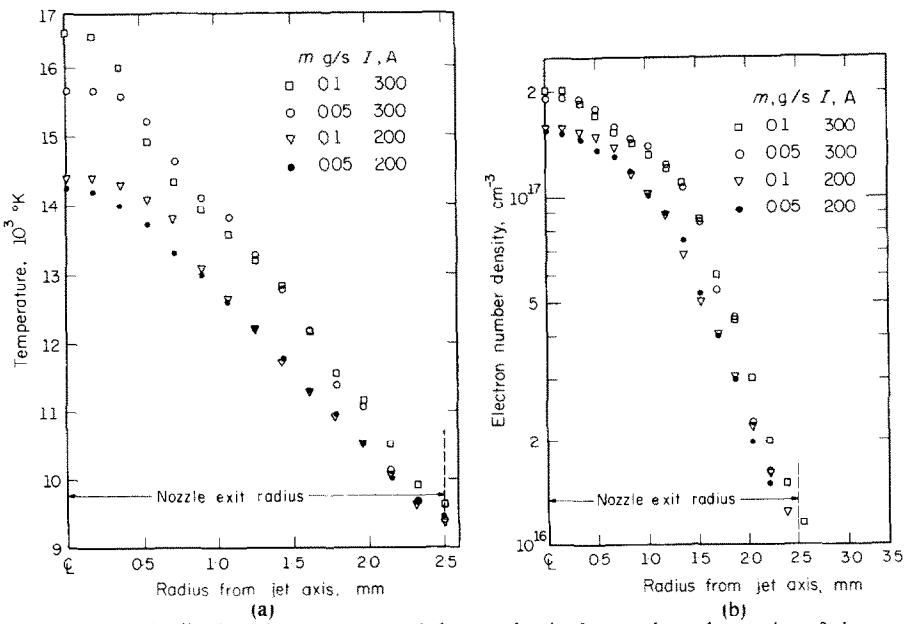

FIG. 6. Radial distribution of temperature and electron density from end-on observation of nitrogen 4955 Å continuum, $P = 1$ atm.
(a) Temperature distribution. (b) Electron density distribution.

sity quickly reached a steady value, and erosion of anode and cathode surfaces was kept at a minimum.

The "end-on" temperature and electron density profiles of the ionized nitrogen are shown in Fig. 6. Because of the optical thinness of the ionized gas, the radiation originated from inside the arc heater at the region of the cathode.

Optical thinness of the "side-on" measurements was checked by placing a second spherical mirror on the far side of the radiating column and focusing the image such that its optical path passed through the gas column twice. Absorption by the gas would result in a decreased intensity seen by the spectrometer; no decrease was observed.

8. ESTIMATION OF PRANDTL NUMBER

Because of small jet velocity, $u_0^* \ll 1$ in the experimental range. The fact that $\sigma = 12$ is correct in magnitude is seen in the plot of equation (7) in Fig. 5 for $N_{Sc} = 1$ and $\sigma = 12$ as well as the cases not shown here. With $\sigma = 12$, the estimated Prandtl number based on equation (9) is shown in Fig. 7. For larger z, the estimated value based on equation (10) is also shown. The closeness of the estimation is shown by the curves in Fig. 4, plotted for various values N_{Pr} from trials. The influence of the parameter σ is seen in that values of N_{Pr} were halved when σ was increased from 12 to 16. However, the trend of N_{Pr} vs. distance remained the same. For large z, the estimation based on equation (10) is also shown in Fig. 4 and the values are included in Fig. 7. N_{Re} was below 200 in all the cases where measurements were made. A comparison to the calculated results of Samaras [23] for air is also shown in Fig. 7 (b).

In a high temperature medium the thermal radiation effect influences the magnitude of N_{Pr}. Figure 7 (b) shows that for the same flow rates in the near jet region, increasing the current from 200 to 300 A decreased the Prandtl

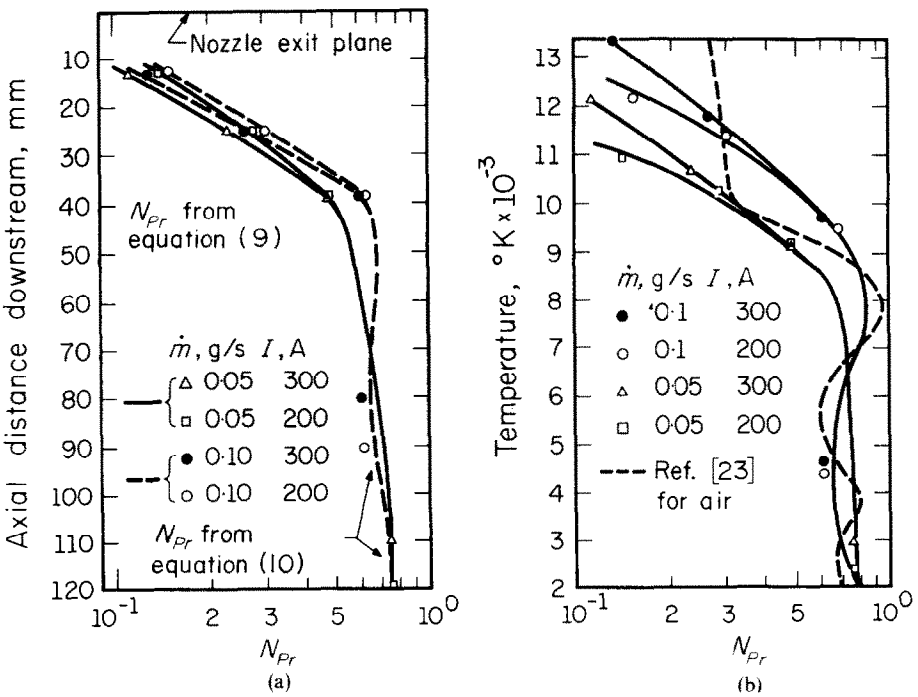

FIG. 7. Prandtl number N_{Pr} of ionized gas in jets, $P = 1$ atm, $\sigma = 12$.
(a) N_{Pr} at various axial locations. (b) N_{Pr} as a function of jet temperatures.

number. Above 10^{4}°K, the trend of N_{Pr} deviates from the theoretical value for air [23] because of large difference in reactivities between nitrogen and air.

The radiation effect [34] which brought about a decreased Prandtl number, widens the thermal jet mixing region. This can clearly be seen in the radial temperature profiles (Fig. 4). Although the increased current input only raised the core temperature slightly, the volume of the high temperature core had increased and the radiation flux from this larger volume effectively reduced the Prandtl number.

9. DISCUSSION

For the axisymmetric jet, the Abel formulation gave the radial intensities as required and the plasma column was experimentally confirmed to have a high degree of transparency for the continuum radiation. The experimental method based on the 4955 Å continuum intensity was shown to be useful.

The major difficulty in this study was the lack of reliable techniques to make measurements in the temperature range $3500°K < T < 9000°K$. This was further complicated by the increasing unsteadiness of the ionized gas column

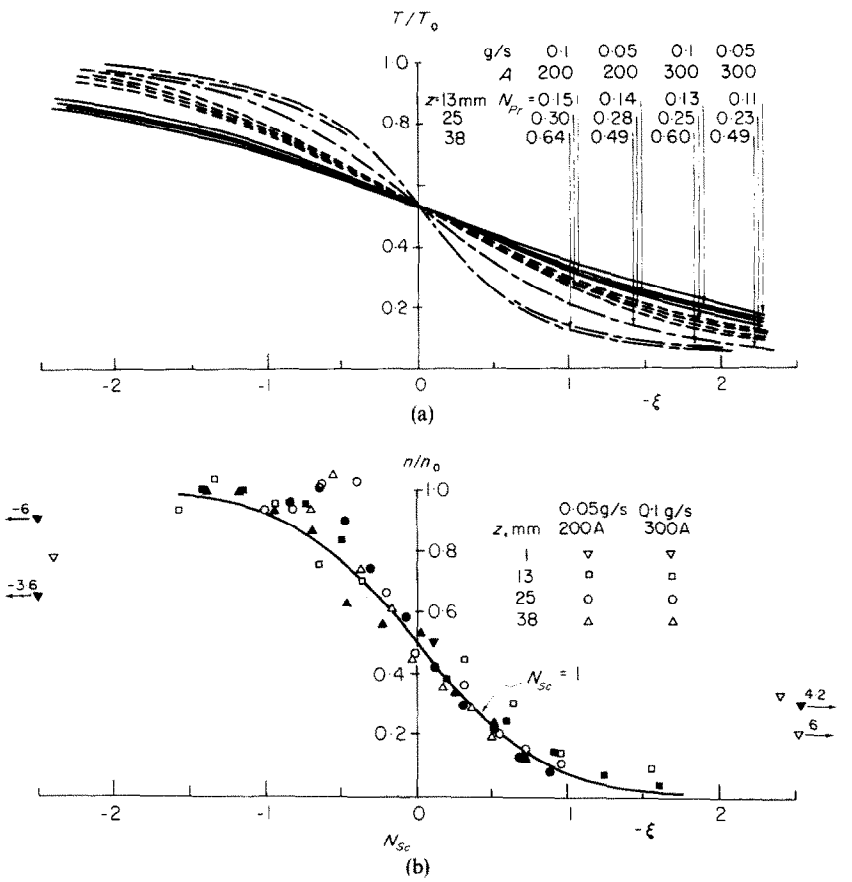

FIG. 8. Dimensionless relations to ξ.
(a) Dimensionless temperature distributions from various sets of data for various Prandtl number. (b) Dimensionless electron density distributions based on Schmidt number of 1 and various sets of data.

at low velocity, as downstream distances increased. The thermocouple traverses to the edge of the high temperature gas served at best to define a rough plume outline.

Temperature and electron density profiles have been experimentally determined in the free jet of ionized nitrogen for mass flow rates of 0·05 and 0·1 g/s at currents of 200 and 300 A. As the temperature in the free jet decreases from an initial value of the order of 14000°K, to room temperature, the Prandtl number increases by an order or magnitude to a room temperature value of about 0·75. More sets of data are presented in [35].

The consistency of the results is seen in the dimensionless plots of temperature and electron density in Figs. 8 (a) and (b) from various sets of experimental data. Figure 8 (a) shows the consistency of trend for the near jet condition as represented by equation (9) with ordinate of T/T_0. Figure 8 (b) shows that the near jet condition of equation (7) is satisfied for a Schmidt number of 1 except at the vicinity of the orifice ($z = 1$ mm). These figures are included for future comparisons. However, it must be noted that the present range of experiments is limited and care must be exercised when extrapolating from these dimensionless correlations.

Over the length of the jet where laminar flow was maintained, steady state was observed at $N_{Re} < 200$, current less than 300 A and flow less than 0·5 g/s. A sudden increase in jet noise was noted at N_{Re} beyond 300. When turbulence occurred and therefore fluctuations in temperature and electron concentration, the present experimental method does not give meaningful results.

Increasing current (which increases the radiation flux) has a greater influence than increasing flow rates on the Prandtl number value in the near jet region. About 10 diameters downstream, the higher mass flow rate appears to cause a more rapid increase of N_{Pr} than the lower flow rate.

ACKNOWLEDGEMENT

The authors wish to thank the National Science Foundation for its support (NSF GK 1195) of this study.

REFERENCES

1. H. R. GRIEM, *Plasma Spectroscopy*, p. 72. McGraw-Hill, New York (1964).
2. D. ROBINSON and D. P. LENN, Plasma diagnostics by spectroscopic methods, *Appl. Optics.* **6**, 983 (1967).
3. E. J. HELLUND, *The Plasma State*, p. 81. Reinhold, New York (1969).
4. E. P. BIALECKE and P. DOUGAL, Pressure and temperature variation of the electron–ion recombination coefficient in nitrogen, *J. Geophys. Res.* **63**, 544 (1958).
5. W. K. MCGREGOR, *Physico-Chemical Diagnosis of Plasmas*, edited by T. H. ANDERSON, pp. 143, 155, 163. Northwestern University Press, Evanston, Il. (1963).
6. A. G. GAYDON, *The Shock Tube in High-Temperature Chemical Physics*, p. 208. Reinhold (1963).
7. H. R. GRIEM, Validity of local thermodynamic equilibrium in plasma spectroscopy, *Phys. Rev.* **131**, 1170 (1963).
8. R. H. HUDDLESTON and S. L. LEONARD, *Plasma Diagnostic Techniques*, pp. 265, 269, 309. Academic Press, New York (1965).
9. A. B. CAMBEL, D. P. DUCLOUS and T. P. ANDERSON, *Real Gas*. Academic Press, New York (1963).
10. C. F. HIRSCHFELDER, R. B. CURTISS and R. B. BIRD, *Molecular Theory of Gases and Liquids*, Chapters 7–11, p. 498. John Wiley (1964).
11. H. N. OLSEN, Partition function and lowering of the ionization potential in an argon plasma, *Phys. Rev.* **124**, 1703 (1961).
12. W. B. KUNKEL, *Plasma Physics in Theory and Application*, p. 300. McGraw-Hill, New York (1966).
13. E. A. MASON and H. W. SCHAMP, Mobility of gaseous ions in weak electric fields, *Ann. Phys., New York* **4**, 233–270 (1958).
14. A. MIRONER and H. MACOMBER, Chemical non-equilibrium effects in thermal arc-jet propulsion, *Prog. Astronaut. Aeronaut.* **9**, 121 (1963).
15. S. T. DEMETRIADES, G. L. HAMILTON, R. W. ZIEMER and P. D. LENN, Three fluid non-equilibrium plasma accelerators. I, *Prog. Astronaut. Aeronaut.* **9**. 461 (1963).
16. S. M. SCALA, Heat transfer in multi-component gases, General Electric Publication, no. R625 D987, p. 35 (December, 1962).
17. E. W. MCDANIEL, *Collision Phenomena in Ionized Gases*, pp. 208, 684. John Wiley, New York (1964).
18. H. SCHLICHTING, *Boundary Layer Theory*, (translated by J. KESTON), pp. 91, 181, 598, 608. McGraw-Hill, New York (1960).
19. S. L. SOO, *Fluid Dynamics of Multiphase Systems*, p. 363. Blaisdell, Waltham, Mass. (1967).
20. H. H. KORST and W. L. CHOW, Non-isoenergetic turbulent jet mixing between two compressible streams at constant pressure, NASA CR-419, pp. 17 (April, 1966).
21. S. L. SOO, Electrohydrodynamic jets, *Proc. 11th Midwestern Mechanics Conference* **5**, 215–244 (Iowa State Univ., Ames, Iowa) (1969).
22. J. B. SCHUMAKER, W. L. WEISE, Measurement of electron density and temperature in dense plasmas by means of line broadening theory, *Temperature*, Vol. **3**, edited by C. M. HERZFELD, pp. 575. Reinhold, New York (1962).

23. D. G. SAMPARAS, *Theory of Ion Flow Dynamics*, pp. 148, 151, 153, 243. Prentice-Hall, Englewood Cliffs, N.J. (1962).
24. M. N. BAHADORI and S. L. SOO, Non-equilibrium transport phenomena of partially ionized argon, *Int. J. Heat Mass Transfer* **9**, 17–34 (1966).
25. B. D. ABCOCK and W. E. G. PLUMTREE, On excitation temperature measurements in a plasma-jet, and transition probabilities for argon lines, *J. Quant. Spectros. Radiat. Trans.* **4**, 29–39 (1964).
26. H. N. OLSEN, Electric arc as a light source for quantitative spectroscopy, *J. Quant. Spectros. Radiat. Transf.* **3**, 305–383 (1963).
27. A. UNSÖLD, *Physik der Sternatmosphären* (Springer-Verlag, Berlin, Germany), 2nd Ed., pp. 90–91 (1955).
28. M. N. BARZELAY, Continuum radiation from partially ionized argon *AIAA Jl* **4**, 815–822 (1966).
29. H. N. OLSEN, Measurement of argon transition probabilities and computation of thermodynamic properties of the argon plasma, *Physico-Chemical Diagnostics of Plasmas*, edited by T. H. ANDERSON, p. 470. Northwestern University Press (1963).
30. K. S. DRELLISHAK, D. P. AESCHLIMAN and A. B. CAMBEL, Tables of thermodynamic properties of argon, nitrogen and oxygen plasmas, Arnold Engineering Development Center, Tenn., AEDC-TDR 64–12 (1964).
31. H. MAECKER, Experimental and theoretical studies of the properties of nitrogen and air at high temperatures, 5th AGARD Colloquium on Combustion and Propulsion, (1963).
32. H. EDELS, K. HEARNE and A. YOUNG, Numerical solutions of the Abel integral equation, *J. Math. Phys.* **41**, 62–75 (1962).
33. C. A. NEEL and C. H. LEWIS, Thermodynamic properties of nitrogen, Arnold Engineering Development Center, Tenn., AEDC-TR-64-113 (1964).
34. S. PAI, *Radiation Gas Dynamics*, p. 143. Springer-Verlag, New York (1966).
35. D. J. MYRONUK, Properties of free jets of ionized nitrogen, Ph.D. thesis, University of Illinois, Urbana (August 1969).

MESURE DE L'AZOTE IONISÉ DANS DES JETS ET ESTIMATION DU NOMBRE DE PRANDTL

Résumé—On réalise par méthode spectroscopique la mesure des températures et des densités d'électrons d'un jet libre d'azote ionisé à la pression atmosphérique. Les températures du gaz sont comprises entre 9000°K et 15000°K et les densités d'électrons entre $5.10^{15}/cm^3$ et $10^{17}/cm^3$. Les débits massiques d'azote varient entre 0,05 et 0,1 gramme par seconde avec des courants d'arc de 200 et 300 A à 40 V. Une estimation des nombres de Prandtl faite à partir de la distribution de température dans le jet conduit à des valeurs comprises entre 0,06 et 0,75.

MESSUNGEN AN IONISIERTEM STICKSTOFF IN DÜSENSTRÖMUNGEN UND ABSCHÄTZUNG DER PRANDTL-ZAHL

Zusammenfassung—Messungen der Temperatur und der Elektronendichte mit Hilfe der spektroskopischen Methode wurden an einem Freistrahl aus ionisiertem Stickstoff bei Atmosphärendruck durchgeführt. Die Gastemperatur bewegt sich im Bereich von 9000 K bis 15000 K, und die Elektronendichte reichte von $5 \cdot 10^{15}/cm^3$ bis $10^{17}/cm^3$. Der Massenstrom des Stickstoffs betrug 0,05 und 0,1 g/s bei einem Lichtbogenstrom von 200 und 300 A und einer Spannung von 40 V. Aus der Temperaturverteilung im Strahl wurde die Prandtl-Zahl geschätzt. Ihr reicht von 0,06 bis 0,75.

ИЗМЕРЕНИЯ НА ИОНИЗОВАННОМ АЗОТЕ В СТРУЯХ И ОЦЕНКА ЧИСЛА ПРАНДТЛЯ

Аннотация—Измерение температур и плоскостей электронов в свободной струе ионизованного азота при атмосферном давлении осуществлялось спектроскопическим методом. Температура изменялась от 9000°К до 15000°К, а плотность электронов от $5 \cdot 10^{15}$ см$^{-3}$ до 10^{17} см$^{-3}$.

Расходы азота составляли 0,05 и 0,1 г/сек при токах дуги 200 и 300 ампер и напряжении 40 вольт. На основании распределения температуры в струе была проведена оценка чисел Прандтля, которая дала значения от 0,06 до 0,75.